JOURNAL OF Applied Polymer SCIENCE

Biopolyamide hybrid composites for high performance applications

Shaghayegh Armioun,[1] Suhara Panthapulakkal,[1] Johannes Scheel,[2] Jimi Tjong,[1] Mohini Sain[1,3]
[1]Center for Biocomposites and Biomaterials Processing, Faculty of Forestry, University of Toronto, Toronto, M5S 3B3, Canada
[2]Department of Mechanics, Faculty of Mechanical Engineering, University of Kassel, Kassel, D-34125, Germany
[3]Center of Excellence for Advanced Materials Research, King Abdulaziz University, Jeddah 21589, KSA
Correspondence to: S. Panthapulakkal (E-mail: s.panthapulakkal@utoronto.ca)

ABSTRACT: This study focuses on the performance characteristics of wood/short carbon fiber hybrid biopolyamide11 (PA11) composites. The composites were produced by melt-compounding of the fibers with the polyamide via extrusion and injection molding. The results showed that mechanical properties, such as tensile and flexural strength and modulus of the wood fiber composites were significantly higher than the PA11 and hybridization with carbon fiber further enhanced the performance properties, as well as the thermal resistance of the composites. Compared to wood fiber composites (30% wood fiber), hybridization with carbon fiber (10% wood fiber and 20% carbon fiber) increased the tensile and flexural modulus by 168% and 142%, respectively. Izod impact strength of the hybrid composites exhibited a good improvement compared to wood fiber composites. Thermal properties and resistance to water absorption of the composites were improved by hybridization with carbon fiber. In overall, the study indicated that the developed hybrid composites are promising candidates for high performance applications, where high stiffness and thermal resistance are required. © 2016 Wiley Periodicals, Inc. J. Appl. Polym. Sci. **2016**, *133*, 43595.

KEYWORDS:

INTRODUCTION

The primary role of environmental regulations is to obligate manufacturers to reduce environmental footprints of their products over their entire life cycle. Lately, the automotive industry has faced major environmental challenges, including a fast-growing petroleum consumption, fuel resource depletion, and an increase in greenhouse gas emissions. These factors call for innovative modifications in automotive designs towards a more sustainable future.[1–3] The main goal of the automotive industry is to reduce vehicles' weight and cost along with enhancing their safety and recyclability after use.[3,4] Furthermore, sustainable development is a popular market trend witnessed in the auto industry, which has given rise to research interests of major automotive companies towards replacing conventional materials with bio-based products as a better environmental friendly alternative. However, the automotive industry is relatively slow in implementing such materials due to the restrictions in choice of materials meeting the high safety and performance requirements.[2,3] Nowadays, there is a fast-growing trend in using natural fibers (biofibers) as reinforcing agents for composites in high performance applications, due to their low cost, light weight, renewability, recyclability, and abundance.[3,5–7]

Over the past few decades, there has been a rising interest in the industrial application of composites consisting of commodity polymers, engineering polymers, and biopolymers reinforced with natural fibers.[2,9] These biocomposites are shown to be good candidates for high performance applications including automotive industry, as they can be modified to meet all the main requirements of the industries.[3,8] Polyamides (PA) are the most widely used engineering polymer matrices in the automotive industry mainly due to their desirable properties, including high thermal stability, good chemical resistance, low flammability, and satisfactory mechanical properties, as well as their low cost and easy handling.[10–14] Among the polyamides, most of the studies were focused on the common petro-based polyamides (PA6 and PA6.6). However, the high melting temperature of these plastics is a drawback while mixing with thermally sensitive natural fibers. [10,13,15–17,20] Polyamide 11 (PA11) is a 100% bio-based polymer and requires relatively low processing temperature (approximately 185 °C),[15–17] which is essential in processing and manufacturing of natural fiber-reinforced composites, due to low thermal stability of natural fibers.[10,13,18–20] This bio-based polyamide has lower density, higher moisture resistance, and lower melting temperature compared to PA 6 and PA 6.6 and is quite new in the automotive industry.[13] In addition, its functional end-groups and amide linkages allow for hydrogen bonding and good interfacial interaction with natural fibers in composite production.[13,15–17] Our aim was to utilize this polymer as a matrix for natural fibers to develop more sustainable high performance biocomposites that can find applications in automotive industry. Feldmann and Bledzki[20] studied the effect of cellulosic fibers as reinforcing agents on other bio-based polyamides (PA6.10 & PA10.10) and reported that properties of the polymer, including

tensile modulus, tensile strength, notched impact strength, energy absorption, and heat deflection temperature were significantly improved by adding cellulosic fibers. However, there are drawbacks associated with natural fibers, including sensitivity to moisture content and high temperature, as well as high level of variability in fiber properties correlated to their cultivating and processing conditions.[7,18]

Carbon fiber is often selected as reinforcement for polymer matrices in high performance applications due to its low weight and excellent mechanical properties.[10,11,14,21,22] The properties of carbon fiber, such as high stiffness, proper tensile strength, good chemical resistance, high-temperature tolerance, and low thermal expansion make it suitable for aerospace and automotive industries.[11,23] Recently, Magniez *et al.*[24] studied short carbon fiber-reinforced PA11 and reported that a small content of carbon fiber could significantly improve PA11 properties, including stiffness, elastic deformation before yield, and creep properties. However, carbon fiber is not renewable and quite expensive compared to other fiber types because of the high consumption of energy in its manufacture. Use of recycled carbon fiber would be definitely a cost-effective alternative for this, which has not been investigated in this study.

Many studies have reported that hybrid composites composed of natural and synthetic fibers can improve the thermo-mechanical properties of the composites by having the advantages of both fiber types in the composite.[5–7] The behavior of hybrid composites is a balance of advantages and disadvantages of each component, in which the advantages of one type of fiber could compensate the lack in the other.[5–7] Hence, hybridization of a small amount of carbon fiber with natural fiber could be another cost-effective alternative for developing high performance biocomposites. The main aim of this study was to develop high performance biocomposites using bio-based polymer (PA11) reinforced with wood fibers and short carbon fibers to be used in automotive applications.

Wood and carbon fibers were hybridized with polyamide11. The total weight fraction of fibers was kept at 30% in all of the composites. Properties of the hybrid composites, such as density, tensile, flexural, impact, and heat deflection (HDT) were evaluated and compared with the non-hybrid composites (wood fiber-reinforced polyamide and carbon fiber-reinforced polyamide). Additional properties, such as scanning electron microscopy (SEM), melt flow index (MFI), and thermal analysis were conducted to investigate the effect of hybridization on the quality and processing of the molded parts.

EXPERIMENTAL

Materials

Rilsan© Polyamide 11 BMNO (density 1.03 g cm^{-3}) was supplied by Arkema. Wood fiber (WF) was supplied by Tembec (density 1.4–1.5 g cm^{-3}) and was pelletized for easy handling and processing during extrusion. The length and diameter of wood fiber used were 0.8 mm and 28 μm on average, respectively, whereas the length and diameter of carbon fiber used were 6 mm and 7 μm on average, respectively. Carbon fiber (CF) was supplied by Zoltek (density 1.81 g cm^{-3}). Maleic anhydride grafted polypropylene (MAPP-G3003) was obtained from Eastman Chemical Company.

Table I. Composition of the Extruded Composite Pellets

Extruded pellets	Wood fiber (wt %) (vol %)	Carbon fiber (wt %) (vol %)	PA11 (wt %) (vol %)	MAPP (wt %)
WF10	10 7	–	86 93	4
WF20	20 15	–	76 85	4
WF30	30 23	–	66 77	4
WF20CF10	20 15	10 6	66 79	4
WF10CF20	10 8	20 13	66 79	4
CF30	–	30 20	66 80	4

Volume fraction of MAPP is included in volume fraction of PA11.

Composite Fabrication

The formulations used for the composite preparation (wt %) as well as components' volume fractions [eqs. (1–3)] are given in Table I. In order to study the effect of wood fiber content on composite properties, different weight fractions of wood fiber (10 − 30 wt %) were used. Four different combinations of wood fiber and carbon fiber were used in the experiment (WF30, WF20CF10, WF10CF20, CF30) keeping the total fiber loading constant at 30 wt %. In all the composite formulations, the amount of MAPP compatibilizer was kept constant at 4 wt %. All the materials were oven-dried at 65 °C overnight in a standard convection oven and were then dried for 2 h at 105 °C prior to extrusion. The pre-dried materials were mixed mechanically prior to extrusion. The samples were extruded using a co-rotating twin extruder (Onyx model TEC, Canada) with screw diameter 25 mm, *L/D* ratio 40:1 and 10 heating zones in the temperature range of 195 − 205 °C. The pelletized extrudates were oven-dried for 2 h at 105 °C prior to injection molding. Standard test specimens for tensile, flexural and impact testing were injection molded (Engel ES-28) according to ASTM D638, D790, and D256 specifications. Injection molding conditions were: injection temperature: 210 °C, injection time: 8 s, cooling time: 38 s, and mold opening time: 2 s.

Material Characterization

Material characterization of polymer, fibers, and composites was carried out to determine and predict the behavior of materials during melt processing and the behavior of the processed composites.

Thermogravimetric Analysis

Degradation characterization of the polymer, fibers, and the composites was carried out using thermogravimetric analysis (TGA). About 10 − 15 mg of the samples were subjected to thermal degradation within a temperature range of ambient temperature to 800 °C in the thermogravimetric Analyzer (TA Instrument Q50, USA) at a heating rate of 10 °C min^{-1} under nitrogen gas flow. The onset of degradation, the temperature at which maximum weight loss rate occurs (T_{max}), and the residue at 800 °C was recorded for comparing the degradation characteristics of the samples studied.

Density

The density of PA11 and composites were measured using ASTM D792 procedure at ambient temperature and was compared with their theoretical densities. The theoretical density of the composite was calculated by the following equations

$$\rho_c = \rho_f V_f + \rho_m V_m, \quad (1)$$

$$V_f = \frac{\frac{w_f}{\rho_f}}{\frac{w_f}{\rho_f} + \frac{w_m}{\rho_m}}, \quad (2)$$

$$V_m = \frac{\frac{w_m}{\rho_m}}{\frac{w_f}{\rho_f} + \frac{w_m}{\rho_m}}, \quad (3)$$

where ρ_c is the composite density, ρ_f and ρ_m are the density of fiber and matrix, respectively, and V_f and V_m, w_f, and w_m are volume fraction and weight fraction of the fiber and matrix, respectively.

The void content of the composites is defined as

$$V_v = \frac{\rho_{ct} - \rho_{ce}}{\rho_{ct}}, \quad (4)$$

where ρ_{ct} is the theoretical density, ρ_{ce} is the experimental density.

Melt Flow Index (MFI)

Melt flow index values of oven-dried neat PA11 and composites were measured using a melt index apparatus (Custom Scientific Instruments Inc.) in accordance with ASTMD1238 at 200 °C under 2.16 kg load. Five replicates were performed for each sample.

Mechanical Properties

Static tensile and flexural properties of injection molded PA11 and composites were measured using a universal testing machine (Instron 3367) according to ASTM standard test methods. Tensile tests were carried out according to ASTM D638 with a span length of 100 mm and a crosshead speed of 12.5 mm min^{-1}. Flexural tests were carried out as per ASTM D790 in three-point loading model at a crosshead speed of 12.5 mm min^{-1} and span width of 50 mm. Izod impact tests were carried out using a digital pendulum impact tester (Tinius Olsen 892) according to ASTM D256. Six specimens for each sample sets were tested for all mechanical testing.

Scanning Electron Microscopy (SEM)

Scanning electron microscopy (Hitachi S-2500, Tokyo, Japan) was used to observe the fracture surfaces of the impact samples under high magnification. Samples were cut carefully to preserve the fracture surfaces. The fracture surface was gold sputtered to avoid electrostatic charge during the examination. Images were taken using an accelerating voltage of 15 kV and a working distance of 10 mm.

Heat Deflection Temperature (HDT)

HDT test was performed to study the behavior of PA11 and composites under stresses at elevated temperatures. The tests were performed according to ASTM D648. Three specimens for each injection molded samples were used in a horizontal position using a calibrated apparatus designed for this purpose (CSI 107-M1-252) with a heating rate of 2 ± 0.2 °C min^{-1} measured by means of a thermocouple. The temperature at a 0.25% deflection of the sample bars under a constant load of 264 psi (1.82 MPa) was recorded as the HDT. After each measurement, the apparatus was cooled down by recirculating water until it reached 20 °C.

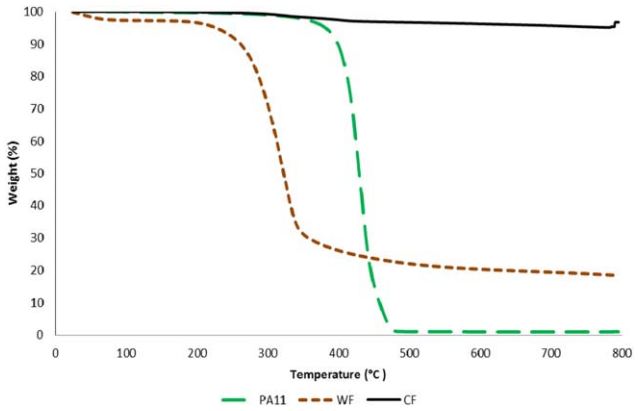

Figure 1. TGA results for neat PA11, wood Fiber (WF), and carbon Fiber (CF). [Color figure can be viewed in the online issue, which is available at wileyonlinelibrary.com.]

Water Absorption/Uptake

Water absorption test was carried out according to ASTM D570-98 (Two-hour Boiling Water Immersion). The percentage of water uptake was calculated by the following equation

$$\text{Water Absorption } (\%) = \frac{W_t - W_0}{W_t} \times 100, \quad (5)$$

Where W_t is the weight of the sample after boiling at time t and W_0 is the initial weight of the sample at $t = 0$.

RESULTS AND DISCUSSION

Thermogravimetric analysis

Thermal degradation characteristics of PA11, wood fibers, and carbon fibers were investigated using TGA. Figure 1 shows the weight loss (%) with rising temperature from room temperature to 800 °C for PA11 and the fibers. The graph shows no considerable weight change for PA11 and carbon fibers from ambient temperature to 200 °C, whereas wood fiber showed about 3% weight loss, indicating the presence of moisture in the wood fiber. According to the TGA profiles, the onset degradation temperature for wood fiber is around 200 °C, followed by the maximum degradation temperature of around 300 °C. Degradation of PA11 occurred between 350 °C and 475 °C. Carbon fiber showed a quite stable profile, with only around 4% decomposed materials, which is more likely correlated to its sizing and coating materials. The important thermal characteristics captured by these plots, including temperatures at 25%, 50% and 75% weight loss, maximum degradation, and residue at 800 °C are extracted in Table II. The results showed the low thermal stability of the wood fiber compared to the polymer and carbon fiber. Wood fiber residue (about 18%) could be from the lignin existing in the wood fiber.

As presented in Figure 2(a), samples WF10, WF20, and WF30 showed quite similar patterns with a two-stage decomposition profile. Compared to PA11, the weight of wood fiber-reinforced

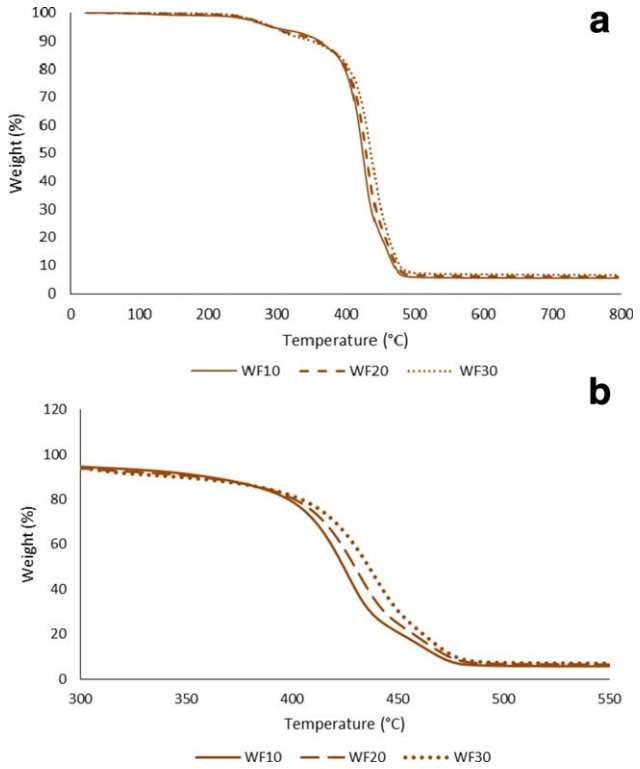

Figure 2. (a) TGA results for wood fiber-reinforced composites (WF10, WF20, and WF30). (b) Shift of the second decomposition temperature of wood fiber-reinforced composites towards higher temperature in detail. [Color figure can be viewed in the online issue, which is available at wileyonlinelibrary.com.]

composites decreased more rapidly with increase in temperature. In the first stage starting at around 200 °C, a weight loss was indicated, which is referred to degradation of wood fiber in the composites. The second decomposition stage, which is correlated to PA11 degradation, began at around 350 °C and followed by the maximum decomposition at around 430 °C. However, it was observed that as the fiber content in the composite increased, the second decomposition temperature was slightly shifted to a higher temperature [Figure 2(b)]. For instance, 50% loss occurred at ~424, 429, and 436 °C for composites WF10, WF20, and WF30, respectively. This might be associated with the high thermal stability of lignin; as the wood fiber content in the composites increased, the lignin content was also increased. It also may suggest a good interaction between wood fiber and polyamide, leading to enhanced thermal properties of the composites.

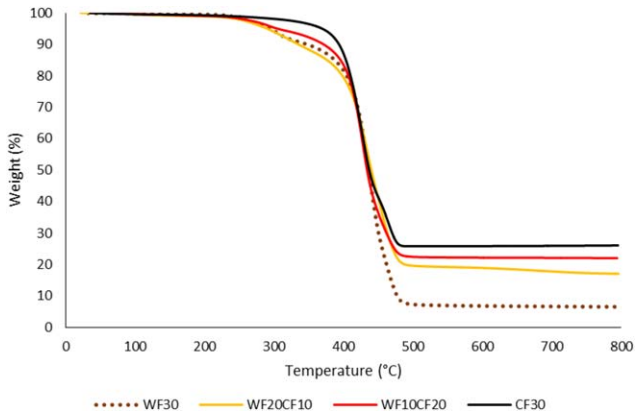

Figure 3. TGA results for composites with 30% fiber content: wood fiber-reinforced (WF30), hybrid (WF20CF10, WF10CF20), and carbon fiber-reinforced (CF30) composites. [Color figure can be viewed in the online issue, which is available at wileyonlinelibrary.com.]

Table II. TGA Results Showing Degradation Temperatures for Neat PA11, Wood Fiber, and Carbon Fiber

Base materials	$T_{25\%}$ (°C)	$T_{50\%}$ (°C)	$T_{75\%}$ (°C)	T_{max} (°C)	Residue after 800 °C (%)
Neat PA11	416	429	441	426	1
Wood Fiber (WF)	295	322	421	318	18
Carbon Fiber (CF)	-	-	-	-	96

Figure 3 represents TGA profiles for composites with 30% reinforcements (WF30, WF20CF10, WF10CF20, and CF30). As shown in Figure 3, hybrid composites (WF20CF10&WF10CF20) showed a two-stage decomposition profile. The two-stage profile represented decomposition of wood fiber at the first stage at around 200 °C, followed by decomposition of PA11 at the second stage at 350 − 430 °C. Carbon fiber did not decompose in the decomposition profiles and increased the residue at the end. Incorporation of carbon fiber decreased the rate of decomposition and enhanced the thermal stability. The degradation profile of hybrid composites indicates their higher thermal stability compared to composite reinforced only by wood fiber, showing that hybridization with carbon fiber enhanced composites thermal performance. The weight percentage at 450 °C was ~30%, 35%, and 40% for wood fiber composite (WF30), hybrid composites (WF20CF10&WF10CF20), and carbon fiber composite (CF30), respectively. Composite CF30, however, showed a one-stage decomposition profile as PA11 degradation profile and almost all the initial carbon fiber content was remained in the leftover, indicating that carbon fiber did not decompose.

Density

The density of material is directly correlated to the weight of automotive part and provides a measure of weight reduction potential with using hybrid biocomposites. Table III represents experimental and theoretical densities of the composites. As expected, the composites' densities slightly increased with rising fiber content. All the experimental densities had lower values compared to the theoretical ones. This might be attributed to the presence of voids in the manufactured composites. The void content has a significant influence on the composite mechanical properties and fatigue strength as it provides greater susceptibility to moisture penetration.[25]

The results indicated that the void content increased with the increase of fiber content in the wood fiber-reinforced composites (WF10, WF20, and WF30). Similar results have been

Table III. Experimental Density vs. Theoretical Density of the Composites

Samples	Experimental density (g mL^{-1})	Theoretical density (g mL^{-1})	Void content (%)
WF10	1.04 ± 0.014	1.06	~1.9
WF20	1.07 ± 0.008	1.10	~2.7
WF30	1.08 ± 0.011	1.14	~5.3
WF20CF10	1.12 ± 0.005	1.15	~2.6
WF10CF20	1.15 ± 0.002	1.17	~1.7
CF30	1.15 ± 0.004	1.18	~2.5

reported by Dhakal, *et al.*[26] on the investigation of hemp fiber-reinforced unsaturated polyester composites. They reported that as the volume fraction of hemp fiber increased, the void content also increased. As shown in Table III, the carbon fiber-reinforced composite (CF30) had lower void content compared to wood fiber-reinforced (WF30) composites and reducing wood fiber content in the hybrid composites lead to a decrease in their void contents. This might be due to the difference in the interfacial adhesion between the wood fibers and the matrix. Wood fibers exist as fiber bundles and during the compounding process these fiber bundles become defibrillated into microfibrils that may remain on the fiber surface or are dispersed in the matrix.[27] The generation of microfibrils increases the surface area of the fibers and this might lead to poor wetting of the fibers with the matrix, which in turn leads to poor interfacial interaction. Among the 30 wt % reinforced composites, the hybrid composite WF10CF20 had the lowest void content (comparable with WF10), showing that incorporation of carbon fiber decreased the porosity problem of the composites to some extent. The lower void content in the hybrid composites indicates good wettability of the fibers with the matrix as well as efficient fibers/matrix adhesions.

Melt Flow Index

Melt Flow Index (MFI) is a measure of the ease of material flow through a die at a specific temperature under a specific load. MFI has been used widely as a material property for any material developed to indicate the processability of the material, especially for processes such as injection molding. The MFI results are presented in Table IV. The MFI for neat PA11 was 18.9 ± 3.9 g (10 min)$^{-1}$. Compared to the neat polymer, the composites showed much lower MFI values, indicating that the presence of fiber reduced the mobility of the polymer molecules under stress. As expected, an increase in fiber content reduced the MFI values. The fibers present in the polymer matrix disturb the dynamics of viscoelasticity of the melt by restricting the mobility of molecular chains and this leads to lower MFI values.[28] The decreasing impact on MFI was more pronounced for wood fiber-reinforced composites, and this could be due to the difference in the microstructure of the two fibers as well as the lower volume fraction of carbon fiber compared to wood fiber at the same weight fraction. The formation of elementary microfibers in wood fibers, during compounding, increases the surface area of the wood fibers and causes further entanglement with the matrix, restricting the mobility of the polymer.[27] This effect does not exist in the carbon fibers, as synthetic fibers such as carbon fibers remain as single fibrils.[27] Hence, a lower MFI value is expected for WF30 composites compared to CF30 composites and the results are as expected (WF30: 2.3 vs. CF30:5.4).

Compared to WF30, incorporation of carbon fiber in the hybrid composite increased MFI by around 239% and 248% for WF20CF10 and WF10CF20, respectively (Table IV). This helps to improve the processability of the hybrid composites. However, CF30 shows lower MFI compared to the hybrid composites. This might be due to the difference in the compatibility of the fibers and the matrix. As mentioned earlier, all the composites contain the same amount of compatibilizer. In the hybrid composites, the compatibilizer might enhance the interaction between wood fibers and polymer rather than increasing the interaction between carbon fiber and the polymer matrix. However, in CF30, the compatibilizer might enhance the interaction between carbon fibers and matrix, restricting the polymer flow, compared to the hybrid composites. Comparison of the SEM images of the composites shows that carbon fibers were much more coated with the polymer matrix in the CF30 composites than the hybrid composites, indicating enhanced interaction of the carbon fibers in the CF30 composites compared to that of the hybrid composites.

Mechanical Properties

Tensile and Flexural Properties. Table V represents tensile and flexural strength and modulus for neat PA11 and wood fiber-reinforced composites. The results showed that tensile and flexural strength of the composites increased with the increase of fiber content. Compared to neat PA11, the tensile strength was improved by from 10% to 22% with the addition of wood fiber from 10 wt % to 30 wt %, while the flexural strength was enhanced by from 15% to 30%. Moreover, compared to PA11, tensile and flexural modulus were improved by from 37% to 71% and by from 26% to 64%, respectively with the addition of wood fiber from 10 wt % to 30 wt % (Table V). As expected, higher wood fiber content resulted in higher tensile and flexural strength and modulus.

Figures 4 and 5 show tensile and flexural strength and modulus for composites with 30% reinforcement (WF30, WF20CF10, WF10CF20, and CF30). The results showed that incorporation of carbon fiber increased the tensile strength for composites

Table IV. MFI for Neat PA11, and the Composites

Sample	MFI for pellets from extrusion g (10 min)$^{-1}$
Neat PA11	18.9 ± 3.9
WF10	8.9 ± 1.6
WF20	4.8 ± 0.6
WF30	2.3 ± 0.3
WF20CF10	7.8 ± 0.4
WF10CF20	8.0 ± 0.7
CF30	5.4 ± 0.9

Table V. Tensile and Flexural Strength and Modulus for Neat PA11 and Wood Fiber-Reinforced Composites (WF10, WF20, WF30)

Sample	Tensile strength (MPa)	Tensile modulus (GPa)	Flexural strength (MPa)	Flexural modulus (GPa)
Neat PA11	35.4 ± 0.8	1.04 ± 0.04	53.5 ± 0.9	1.10 ± 0.02
WF10	38.8 ± 0.5	1.41 ± 0.01	61.4 ± 0.7	1.39 ± 0.02
WF20	40.0 ± 1.2	1.61 ± 0.07	66.8 ± 0.7	1.64 ± 0.04
WF30	43.3 ± 0.5	1.78 ± 0.02	69.9 ± 0.8	1.80 ± 0.03

WF20CF10, WF10CF20, and CF30 by 36%, 65%, and 105%, respectively, compared to WF30 (Figure 4). The flexural strength was improved by 41% and 73% for hybrid composites WF20CF10 and WF10CF20, respectively, and by 103% for composite CF30, compared to WF30 (Figure 4).

In hybrid composites, as the carbon fiber content increased, the tensile and flexural strength of the composites enhanced. A similar trend has been observed for tensile and flexural modulus of the composites which could possibly be due to higher strength and modulus of carbon fiber. Tensile modulus for the hybrid composites WF20CF10 and WF10CF20 was improved by 79% and 168%, respectively (Figure 5). The flexural modulus for WF20CF10 and WF10CF20 was enhanced by 75% and 142%, respectively (Figure 5). Compared to WF30, tensile and flexural modulus of CF30 enhanced by 203% and 204%, respectively (Figure 5). The results showed that incorporation of carbon fiber improved the tensile and flexural properties (strength and modulus) of the composites, owing to the excellent mechanical properties of carbon fiber. The results also represented a fairly good fiber-matrix adhesion, resulting in a good transferring of the applied load from the matrix to the fibers. Similar results have been reported by Magniez *et al.*[24] for carbon fiber-reinforced PA11.[24]

Impact Properties. Impact strength is a measurement of the material ability to resist the fracture failure under stress applied at high speed and is directly correlated to the composite toughness. It represents the energy required for crack propagation via a notch or any deformation in a material (notched impact strength). Impact strength is one of the undesirable weak points of natural fiber-reinforced composites.[6,29] Impact strengths of neat PA11 and composites were measured using notched and unnotched Izod impact testing. Table VI shows the notched and unnotched Izod impact strength for neat PA11 and wood fiber-reinforced composites. Notched impact tests showed strengths for neat PA11 at 73 ± 12 J m^{-1}; however, adding wood fiber decreased the impact strength significantly. The increase in wood fiber content did not have much effect on the notched impact strength. Figure 6 represents the notched impact strength for composites with 30% reinforcement. As shown in Figure 6, incorporation of carbon fiber in the composites improved notched impact strength to some extent. The highest notched impact strength was represented by composite CF30 at 88.35 ± 3 J m^{-1}, which was improved by about 20% compared to neat PA11. Compared to WF30, hybridization with carbon fiber increased the notched impact strength of the composite WF20CF10 and WF10CF20 by 9% and 88%, respectively (Figure 6).

As shown in Table VI, the unnotched impact strengths of the wood fiber composites are lower than that of neat PA11. The neat PA11 did not fracture during unnotched impact test and exceeded the machine limit of 750 J m^{-1}. Composite WF10 represented an unexpectedly high value of unnotched impact strength, which might be associated with the low fiber content of the composite (10% WF). The low fiber content of the composite could result in matrix dilution, which makes the composite's performance quite similar to its matrix. Figure 7 represents the unnotched impact strength for the composites with 30% reinforcement. Compared to WF30, hybridization with carbon fiber increased the unnotched impact strength of the composite WF20CF10 and WF10CF20 by 46% and 77%, respectively (Figure 7). In general, adding carbon fiber increased

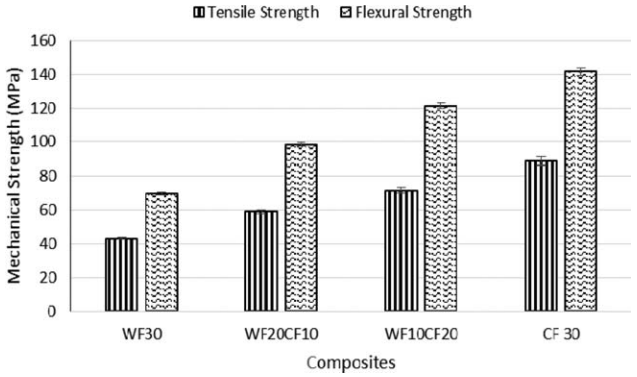

Figure 4. Tensile and flexural strength for composites with 30% fiber content: wood fiber-reinforced (WF30), hybrid (WF20CF10, WF10CF20), and carbon fiber-reinforced (CF30) composites.

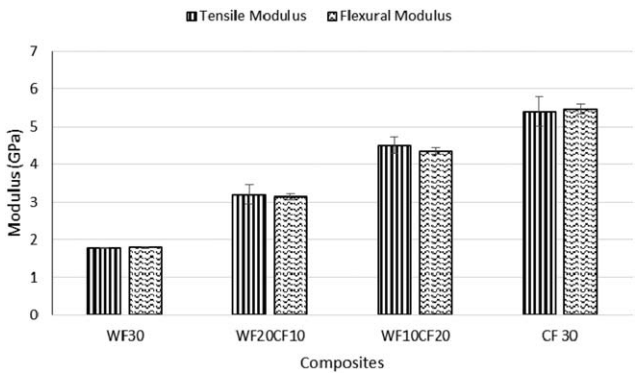

Figure 5. Tensile and flexural modulus for composites with 30% fiber Content: wood fiber-reinforced (WF30), hybrid (WF20CF10, WF10CF20) and carbon fiber-reinforced (CF30) composites.

Table VI. Impact Strength for Neat PA11, and Wood Fiber-Reinforced Composites (WF10, WF20, WF30)

Sample	Notched impact strength (J m^{-1})	Unnotched impact strength (J m^{-1})
Neat PA11	73.0 ± 12	>750
WF10	21.6 ± 0.83	430 ± 82
WF20	22.4 ± 0.75	227 ± 36
WF30	23.9 ± 0.91	228 ± 39

the unnotched impact strength of the composites. Consequently, hybridization with carbon fiber improved both notched and unnotched impact strengths. Proper interfacial strength between fibers and matrix may result in an increase in impact strength in hybrid biocomposites. However, incorporation of two dissimilar fibers may also lead to a non-uniform distribution of fibers in the matrix. The impact strength still needs to be improved for high performance structural applications.

Scanning Electron Microscopy (SEM)

The fracture surfaces of the impact test samples were observed by SEM (Figure 8). SEM is a promising instrument to study fiber-matrix interaction and fracture performance of composites. The figures show effective fiber/matrix interfacial bonding with efficient component integration and good fiber dispersion. No matrix cracking was observed in any of the composites. Proper interfacial bonding resulted in an efficient stress transfer from matrix to the fiber and fiber fracture indicated that applied stress exceeded the fiber strength. With increasing fiber content, voids were observed on the fracture surfaces due to the lack of a proper interfacial bonding between fiber and matrix. This is consistent with density test results, in which as fiber content increased, void content increased. Fiber pullout was more pronounced for composites reinforced with carbon fiber (WF20CF10, WF10CF20, and CF30). In general, fiber breakage was probably the dominant fracture mechanism in wood fiber composites; however, carbon fiber-reinforced and hybrid composites were governed by both fiber pullout and fiber breakage mechanisms.

Heat Deflection Temperature

Heat deflection temperature, also known as heat distortion temperature, is a measure of the upper boundary for the dimensional stability of the materials under a particular load at elevated temperature. This thermomechanical property predicts the stiffness variation of the materials at elevated temperatures and defines the temperature at which a specified degree of deflection occurs owing to a set loading condition. It is an important material property considered when choosing materials for high performance applications.

The HDT values for neat PA11 and the composites are shown in Figure 9. The HDT for neat PA11 was 44 °C, and there was no improvement observed in HDT of composite WF10. By increasing wood fiber content, a slight improvement in HDT for composites WF20 and WF30 was observed. However, incorporation of carbon fiber resulted in much higher HDT values. The maximum HDT value was for composite CF30 at 142 °C, which is significantly higher than the HDT of neat PA11 and wood fiber-reinforced composites (WF10, WF20, and WF30). As shown in Figure 9, hybridization with carbon fiber improved the HDT values for the composites WF20CF10 and WF10CF20 by 106% and 159%, respectively, compared to WF30. This result suggests that these hybrid biocomposites have potential to be applied where maximum service temperature requirement is below 130 °C.

Water Absorption/Uptake

Water absorption is an undesirable problem in natural fiber-reinforced composites due to the moisture sensitivity of the natural fibers. Water uptake behavior is extremely accelerated at elevated temperatures, resulting in significant decrease in mechanical properties related to the degradation of the fiber-matrix interface.[6,7,26] Besides, water absorption can cause swelling, leading to dimensional variation in the composites.[30] Water uptake increases with rising fiber volume fraction due to increased void contents.

Figure 10 represents water absorption for neat PA11 and the composites. The results indicate that adding wood fiber increased water absorption of the composites. As expected, with increasing wood fiber content in the composites, water absorption also increased. The highest water absorption is for WF30,

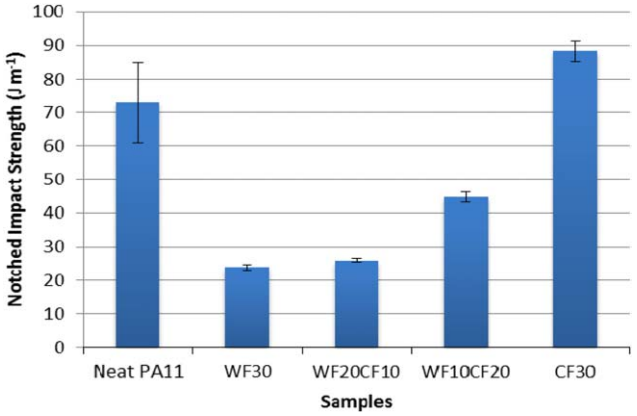

Figure 6. Notched impact strength for composites with 30% fiber content: wood fiber-reinforced (WF30), hybrid (WF20CF10, WF10CF20), and carbon fiber-reinforced (CF30) composites. [Color figure can be viewed in the online issue, which is available at wileyonlinelibrary.com.]

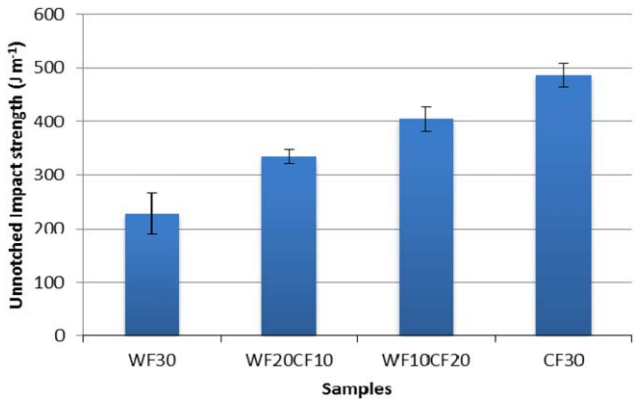

Figure 7. Unnotched impact strength for composites with 30% fiber content: wood fiber-reinforced (WF30), hybrid (WF20CF10, WF10CF20), and carbon fiber-reinforced (CF30) composites. [Color figure can be viewed in the online issue, which is available at wileyonlinelibrary.com.]

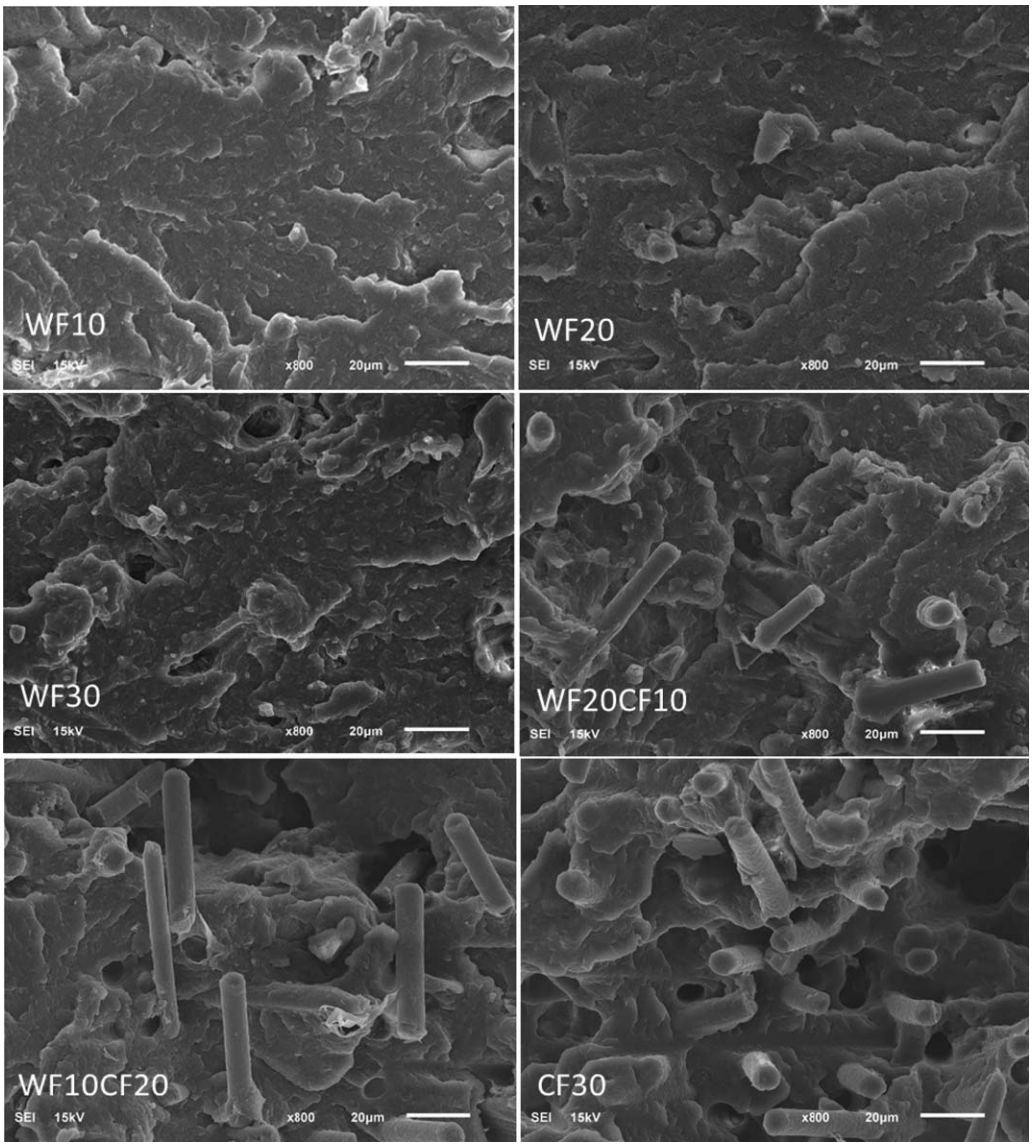

Figure 8. SEM images of fracture surface of the composites WF10, WF20, WF30, WF20CF10, WF10CF20, and CF30 at 800×.

in which the water absorption was increased by 70% compared to neat PA11 (Figure 10). The reported values in Figure 10 indicated that incorporation of carbon fiber in wood fiber composites decreased their water absorption. Compared to WF30, the water uptake for WF20CF10 and WF10CF20 was reduced by 18% and 52%, respectively (Figure 10). Reducing wood fiber content from 20 wt % to 10 wt % in hybrid composites (WF20CF10 to WF10CF20) resulted in lower water uptake. The lowest water absorption was observed for CF30 due to the absence of wood fiber in the composites.

CONCLUSIONS

This paper has demonstrated wood/carbon fiber hybrid biocomposites with a balance between thermal stability, tensile, flexural, impact, heat deflection, and flow properties required for high performance application, such as automotive structural applications. Incorporation of carbon fiber in wood fiber composites

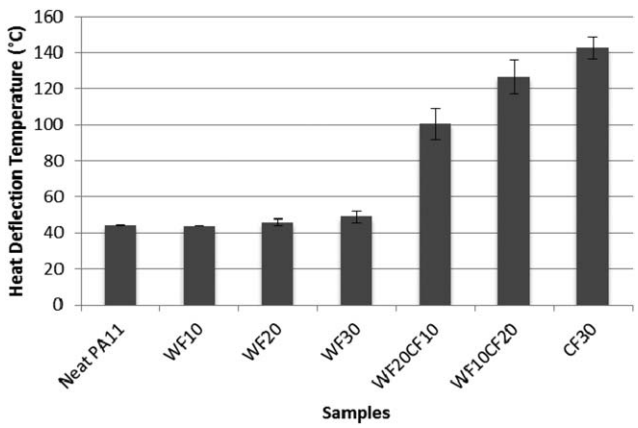

Figure 9. HDT for composites: wood fiber-reinforced (WF10, WF20, WF30), hybrid (WF20CF10, WF10CF20), and carbon fiber-reinforced (CF30) composites.

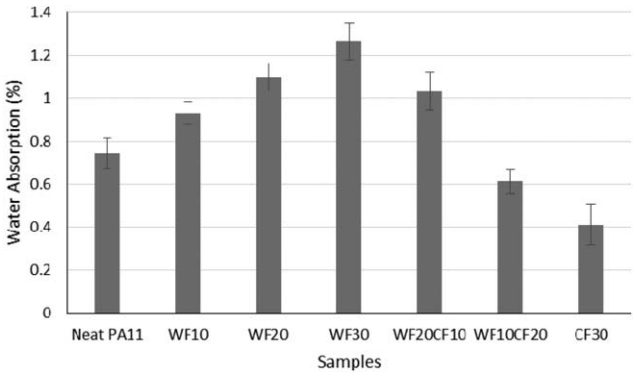

Figure 10. Water absorption for composites: wood fiber-reinforced (WF10, WF20, WF30), hybrid (WF20CF10&WF10CF20), carbon fiber-reinforced (CF30) composites.

improved their mechanical and thermal properties. Tensile and flexural strength and modulus, as well as heat deflection temperature and thermal stability of the composites were enhanced by replacing a fraction of wood fiber with carbon fiber. Compared to neat PA11, impact strength was generally reduced in the composites; however, it was dramatically improved by hybridization with carbon fiber. The moisture uptake was also decreased by incorporation of carbon fiber in the hybrid composites. In overall, this study shows hybridization of synthetic fibers such as carbon fiber makes natural fiber composites more suitable for high performance applications. Understanding the effect of void and the fiber content as well as improvement of impact strength will be the future directions of this study.

ACKNOWLEDGMENTS

The authors would like to acknowledge the financial support from the NSERC Automotive Partnership Canada (APC) program and the in-kind support from the industrial partners FORD Motors Canada for this research. Technical help from Shiang Law is also greatly acknowledged.

REFERENCES

1. Oksman, N. K.; Sain, M., Eds.; In Wood-Polymer Composites; Cambridge: Woodhead Publishing: **2008**.
2. Faruk, O.; Bledzki, A. K.; Fink, H.; Sain, M. *Prog. Polym. Sci.* **2012**, *37*, 1552.
3. Faruk, O.; Bledzki, A. K.; Fink, H.; Sain, M. *Macromol. Mater. Eng.* **2014**, *299*, 9.
4. Vaidya, U. In Composites For Automotive, Truck, and Mass Transit: Materials, Design, Manufacturing; DEStech Publications: Lancaster, **2011**.
5. Panthapulakkal, S.; Law, S.; Sain, M. In International SAMPE Technical Conference, **2005**.
6. Panthapulakkal, S.; Sain, M. *J. Appl. Polym. Sci.* **2007**, *103*, 2432.
7. Panthapulakkal, S.; Sain, M. *J. Compos. Mater.* **2007**, *41*, 1871.
8. Bledzki, A. K.; Faruk, O.; Sperber, V. E. *Macromol. Mater. Eng.* **2006**, *291*, 449.
9. Holbery, J.; Houston, D. *JOM* **2006**, *58*, 80.
10. Botelho, E. C.; Figiel, L.; Rezende, M. C.; Lauke, B. *Compos. Sci. Technol.* **2003**, *63*, 1843.
11. Nie, W. Z.; Li, J. *Plast. Rubber. Compos.* **2010**, *39*, 10.
12. Grozdanov, A.; Bogoeva-Gaceva, G. *J. Thermoplas. Compos.* **2010**, *23*, 99.
13. Kuciel, S.; Kuzniar, P.; Liber-Knec, A. *Polymers* **2012**, *57*, 627.
14. Karsli, N. G.; Aytac, A. *Compos. Part B* **2013**, *51*, 270.
15. Kohan, M. I.; Mestemacher, S. A.; Pagilagan, R. U.; Redmond, K. In Polyamides in Ullmann's Encyclopaedia of Industrial Chemistry, 7th ed., Wiley-VCH Verlag GmbH & Co. KGaA, **2007**.
16. Shen, L.; Worrell, E.; Patel, M. *Biofuels. Bioprod. Bior.* **2010**, *4*, 25.
17. Brehmer, B. In Bio-based Plastics; Wiley & Sons Ltd, **2013**; pp 275–293.
18. Mohanty, A. K.; Misra, M.; Drzal, L. T. *J. Polym. Environ.* **2002**, *10*, 19.
19. Oksman, K.; Mathew, A. P.; Sain, M. *Plast. Rubber. Compos.* **2009**, *38*, 396.
20. Feldmann, M.; Bledzki, A. K. *Compos. Sci. Technol.* **2014**, *100*, 113.
21. Donnet, J. In Carbon Fibers, 3rd ed.; Marcel Dekker: New York, **1998**.
22. Morgan, P. In; Carbon Fibers and Their Composites. Boca Raton: Taylor & Francis: **2005**.
23. Nairn, J. A. In Bascom, W. D.; Harper, S. I., Eds.; Langley Research Center, Effects of Fiber, Matrix, and Interphase on Carbon Fiber Composite Compression Strength. Hampton, Va: Langley Research Center: **1994**.
24. Magniez, K.; Iftikhar, R.; Fox, B. L. *Polym. Compos.* **2015**, *36*, 668.
25. De Almeida, S. F. M.; Neto, Z. dS. N. *Compos. Struct.* **1994**, *28*, 139.
26. Dhakal, H. N.; Zhang, Z. Y.; Richardson, M. O. W. *Compos. Sci. Technol.* **2007**, *67*, 1674.
27. Sain, M.; Panthapulakkal, S.; Law, S. US Patent 8940132 January 27, (**2015**).
28. Ota, W. N.; Amico, S. C.; Satyanarayana, K. G. *Compos. Sci. Technol.* **2005**, *65*, 873.
29. Ranganathan, N.; Oksman, K.; Nayak, S. K.; Sain, M. *J. Appl. Polym. Sci.* **2015**, *132*,
30. Nabi Saheb, D.; Jog, J. P. *Adv. Polym. Technol.* **1999**, *18*, 351.